HAYATI
Journal of Biosciences

Vol. 32 No. 6, November 2025 1426-1436
DOI:10.4308/hjb.32.6.1426-1436
ISSN: 1978-3019
EISSN: 2086-4094

Research Article

Check for updates

OPEN ACCESS

Quantitative Analysis of hsa-miR-21-5p Expression in Human Umbilical Cord Mesenchymal Stem Cell-derived Exosomes Under Hypoxia

Daisy Ramadhani Muhammad[1], Anggraini Barlian[1,3*], Harry Murti[2], Matheus Alvin Prawira[2], Naufalia Faza[2]

[1]*School of Life Sciences and Technology, Institut Teknologi Bandung, Bandung 40132, Indonesia*
[2]*Stem Cell and Cancer Institute, PT Kalbe Farma, Tbk., East Jakarta 13210, Indonesia*
[3]*Scientific Imaging Center (SIC) ITB, Institut Teknologi Bandung, Bandung 40132, Indonesia*

ARTICLE INFO

Article history:
Received December 10, 2024
Received in revised form March 8, 2025
Accepted May 28, 2025
Available Online July 23, 2025

KEYWORDS:
enrichment,
exosome,
hsa-miR-21-5p,
hypoxia,
qRT-PCR

ABSTRACT

Exosomes have emerged as a cell-free alternative to mesenchymal stem cells (MSCs). Hypoxic preconditioning might result in the production of exosomes with ideal properties. As such, the effect of hypoxia on hsa-mir-21-5p expression, which is known to contribute to the immunomodulatory activity of exosomes, should be investigated. This research aimed to enrich and characterize exosomes from human umbilical cord MSC (hUC-MSC) secretome samples secreted under hypoxia and normoxia, as well as to analyze the expression of hsa-miR-21-5p in each sample. Secretomes were collected from cultured cells under both hypoxic and normoxic conditions, and exosomes were subsequently enriched from the secretomes through ultrafiltration. In this research, it was found that particles in N-Exo and H-Exo exhibited round morphology, expressed exosomal CD81 and CD63 markers with an average size of 153.7 ± 31.3 nm and 137.7 ± 25.0 nm, respectively. N-Exo and H-Exo can also be internalized by mesenchymal stem cells (MSCs). qRT-PCR results then indicated that hsa-miR-21-5p expression was significantly lower in H-Exo ($p < 0.05$). In conclusion, hypoxic preconditioning, as performed in this research, was also found to affect hsa-miR-21-5p and downregulate its expression in hypoxic samples relative to controls.

1. Introduction

Within the last two decades, epidemiological studies have revealed a significant increase in inflammatory diseases and its prevalence is expected to continue to rise for the next 30 years (Ji *et al*. 2016) However, conventional approaches in managing inflammatory diseases involves the use of anti-inflammatory and immunosuppressive drugs which possesses several drawbacks such as toxicity and drug resistance (Tabas & Glass 2013) as well as an increased risk of infection due to prolonged suppression of the immune system (McCaughan 2004). Therefore, other therapeutic agents, such as mesenchymal stem cells (MSCs), have been widely studied as an alternative treatment method due to their ability to modulate the immune system without the side effects associated with conventional drugs (Regmi *et al*. 2019).

As a therapeutic agent for the treatment of inflammatory diseases, MSCs primarily act by producing immunomodulatory factors that influence neighboring cells and the progression of inflammation (Wang *et al*. 2014). These MSC secretions comprise a diverse array of molecules, including cytokines, growth factors, and miRNA (Giovannelli *et al*. 2023). The use

* Corresponding Author
E-mail Address: aang@itb.ac.id

of these secreted factors even without the MSCs itself was shown to effectively treat inflammatory diseases such as multiple sclerosis in animal models (Bai *et al*. 2012) This knowledge has led to a growing focus on the potential of harnessing the MSC secretome or its components as opposed to utilizing the MSC itself as a therapeutic agent.

Among the factors contained in the MSC secretome are exosomes. Exosomes are a type of extracellular vesicle (EV) that ranges in size between 30 and 150 nm and is secreted by cells through the endosomal pathway as a form of intercellular communication (Théry *et al*. 2018). These vesicles are now widely studied due to their potential for use in cell-free therapies, including those aimed at treating inflammatory diseases (Harrell *et al*. 2019). Exosomes can mimic the immunomodulatory properties of MSCs, making them more practical to produce and store. Exosomes also possess a lipid bilayer membrane, which serves to protect the cargo they contain, thereby increasing their bioavailability and stability compared to other dissolved components in the MSC secretome (Cha *et al*. 2018). In addition, MSC-derived exosomes, like MSCs themselves, are also capable of homing to inflamed tissues (Harrell *et al*. 2019). Their small size is also another advantage, allowing them to be safely administered through the circulatory system (Cha *et al*. 2018). The safety of exosomes is also reflected in their hypoimmunogenic nature, which enables them to evade immune rejection despite being allogenic due to the lack of expression of class I or II MHC molecules on their surface (Hou *et al*. 2021). Thus, MSC-derived exosomes are similar to MSCs in terms of their immunomodulatory and homing capacities, but with the added advantages of easier production and storage, as well as a superior safety profile.

The therapeutic effect of MSC-derived exosomes in the context of cell-free therapy is primarily mediated by the cargo they carry, namely bioactive molecules such as metabolites, lipids, proteins, and various types of RNA species produced by MSCs (Harrell *et al*. 2019). Among the many functional cargos contained in MSC exosomes, miRNAs are reported to play a crucial role in regulating the inflammatory response by modulating the expression of specific inflammatory factors (Soler-Botija *et al*. 2022). hsa-miR-21-5p has been referred to as a key switch in the transition to an anti-inflammatory response (Sheedy 2015) due to its ability to regulate the expression of its target genes PDCD4, PTEN, and GSK3β, which collectively result in a reduction of TNFα production and an increase in IL-10 production. hsa-miR-21-5p has been extensively discussed in the context of inflammatory diseases and has been found to alleviate several disease models, ranging from periodontitis (Zhou *et al*. 2018) to myocardial infarction (Yang *et al*. 2018) and acute kidney failure (Song *et al*. 2018). Thus, hsa-miR-21-5p can be said to be one of the cargoes with a dominant role within MSC-derived exosomes, given its immunomodulatory capacity.

Exosomes and their cargoes are inherently products of their source cells and consequently sensitive to the microenvironment, which can affect the function and condition of these cells (Zhang *et al*. 2021). *In vivo*, MSCs are found in hypoxic niches with oxygen saturation levels ranging from 2% to 9%. Hypoxic conditions are thus a component of the MSC microenvironment that plays a role in maintaining its function and identity. Whereas *in vitro*, MSCs are commonly cultured under various conditions, specifically with an oxygen saturation level of 21% (Nowak-Stępniowska *et al*. 2022). Therefore, hypoxia conditioning can enable MSCs to be exposed to oxygen saturation levels similar to those in their *in vivo* niches, thereby triggering the production of exosomes with more ideal biological functions. This may then be reflected in the expression of hsa-miR-21-5p. Therefore, this present study aimed to characterize exosomes derived from hUC-MSCs cultured under hypoxic and normoxic conditions (henceforth referred to as H-Exo and N-Exo) and to determine the expression levels of hsa-miR-21-5p in H-Exo relative to those in N-Exo.

2. Materials and Methods

2.1. Cell Culture and Secretome Production

Secretomes were produced as previously optimized by Pranata with slight modifications. Secretomes were sourced from hUC-MSC cells cultured in MEM-α (Gibco, 32561-102) supplemented with 5% human platelet lysate (AventaCell, HPCFDCGL50). Cells were cultured until the 5th passage in a tri-gas incubator (HERAcell Bios 160i) under normoxia (20% O_2, 5% CO_2) and hypoxia (5% O_2, 5% CO_2). Secretomes were collected after 24, 48, and 72 hours of incubation, pooled, and stored at -80°C before use.

2.2. Exosome Enrichment

Exosomes were enriched from secretomes through ultrafiltration. Secretomes were filtered through 0.20 µm filters (Corning, 431229), and the filtrates were centrifuged at 3500g at 4°C using Amicon Ultra-15 Centrifugal Filter Units with a 100 kDa cutoff (Millipore, UFC910008) to remove constituents smaller than 100 kDa, such as proteins and free nucleic acids. Retentates were then further processed through diafiltration with phosphate-buffered saline (PBS). A 20× concentrated solution of Normoxic and Hypoxic exosomes was obtained by ultrafiltration of secretomes and stored at -80°C until further use.

2.3. Exosome Characterization

To verify the presence of exosomes within samples, characterization of exosomes was conducted in accordance with the recommendations of ISEV and other relevant studies. Exosome samples were tested for exosomal tetraspanin marker proteins, CD81 and C63, through western blotting with anti-CD81 (Abcam, ab92726) and anti-CD63 (Santa cruz, sc5275) antibodies. Equal protein loading was confirmed through ponceau staining. Characterization was further carried out by visualization through transmission electron microscopy (TEM) using the Hitachi HT7700, determination of size distribution through dynamic light scattering (DLS) using a Horiba SZ-100 instrument, and particle quantification by nanoparticle tracking analysis (NTA) with a Viewsizer Horiba Type 3000/0053 instrument. To further support characterization, the internalization of exosomes was also assessed through labeling exosomes with the PKH67 Green Fluorescent Cell Linker Kit (Merck, MINI67-1KT) according to the manufacturer's protocol and qualitative observation using an Olympus Fv1200 Confocal Laser Scanning Microscope after an incubation period of one hour.

2.4. RNA Isolation and Quantitative Real-time Polymerase Chain Reaction (qRT-PCR)

Total RNA was extracted from N-Exo and H-Exo using the Plasma/Serum Circulating and Exosomal RNA Purification Kit (Norgen Biotek) according to manufacturer protocol, and A260/280 ratio was assessed using NanoDrop™ One. RNA quantity was assessed using Qubit™ 3 Fluorometer. Total RNA was stored at -80°C until further use. cDNA synthesis was performed using a TaqMan® Advanced miRNA cDNA Synthesis Kit (Applied Biosystems) or TaqMan™ MicroRNA Reverse Transcription Kit (Applied Biosystems) with a Veriti™ thermal cycler instrument. Real-time PCR was performed using the TaqMan protocol with a StepOne™ Real-Time PCR instrument, and relative miRNA expression levels were calculated using the $2^{-\Delta\Delta Ct}$ method with hsa-miR-191-5p and hsa-miR-423-5p as endogenous controls. The TaqMan Assay IDs were: hsa-miR-21-5p (477975_mir); hsa-miR-423-5p (002340); hsa-miR-191-5p (002299).

2.5. Statistical Analysis

Independent samples T-Tests were carried out using IBM SPSS (SPSS, Inc.) with a 95% confidence interval to determine statistical significance.

3. Results

3.1. Characterization of N-Exo and H-Exo

To characterize exosomes, three replicates of N-Exo and H-Exo samples were tested for exosomal surface markers through western blotting. As shown in Figure 1, CD81 and CD63 bands of similar intensities can be observed in all three replicates of N-Exo and H-Exo. The visualization results, as presented in Figure 2, show the presence of morphologically round and oval structures measuring 30-40 nm in each sample.

DLS was conducted on N-Exo and H-Exo samples to ascertain the size distribution of particles within the samples. The Z-average and polydispersity index (PI), along with the size distribution of each sample, were obtained from the DLS readings and are summarized in Table 1. As depicted in Figure 3A, the Z-average of N-Exo and H-Exo particles did not differ significantly. NTA analysis was carried out on one representative sample of N-Exo and H-Exo, each, in order to obtain the frequency of each exceptionally sized particle in the sample. NTA readings were then used to determine the exosome concentrations in the samples, as shown in Table 2. As shown in Figure 4, 36.2% and 42.6% of particles within N-Exo and H-exo samples, respectively, fall within the exosomal size range (30-150 nm). This size range is because exosomes are specifically extracellular vesicles (Evs) secreted through the endosomal pathway. Qualitative observation of both N-Exo and H-Exo samples through confocal microscopy, as depicted in Figure 5, shows the presence of PKH67-labelled exosomes within the cytosolic region of hWJ-MSC cells.

3.2. Hsa-miR-21-5p Expression in H-Exo Relative to Expression in N-Exo

After the presence of exosomes within N-Exo and H-Exo samples was confirmed through the characterization steps discussed previously, the expression of hsa-miR-

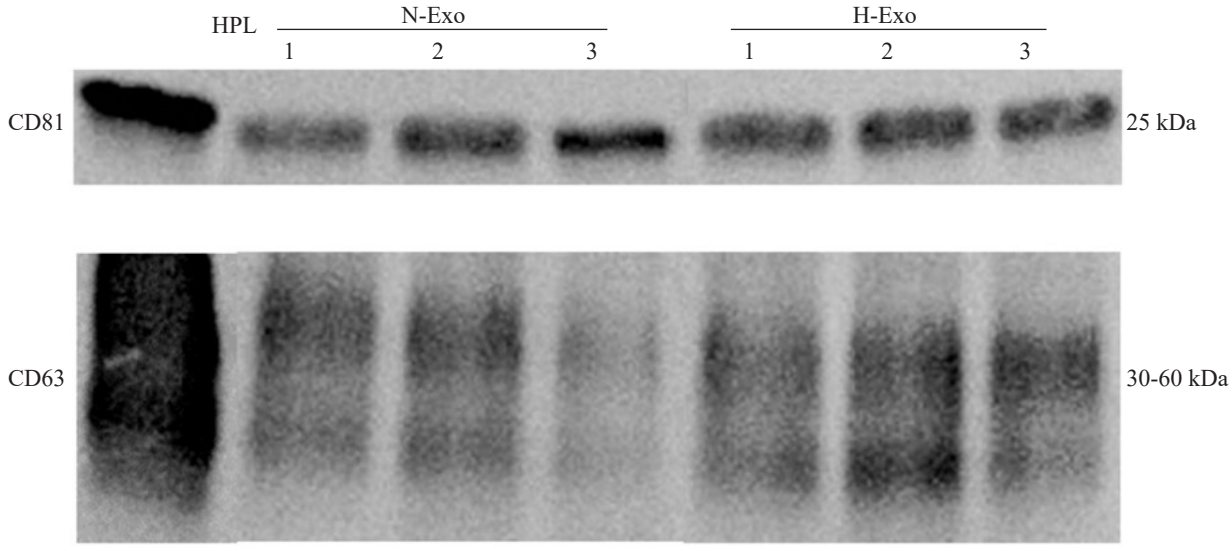

Figure 1. Western blot results of three replicates of N-Exo and H-Exo samples. HPL (human platelet lysate) presented as positive control

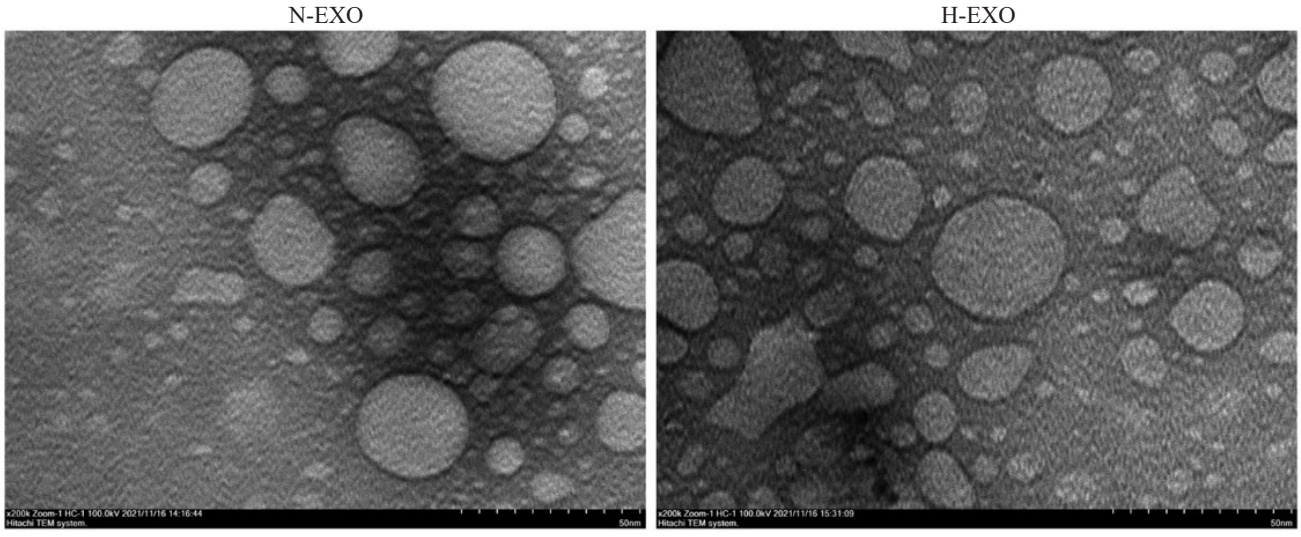

Figure 2. TEM images of N-Exo and H-Exo negatively stained with uranyless dye

Table 1. Dynamic light scattering (DLS) readings of N-Exo and H-Exo

Sample	Z-average	Polydispersity index	Peak (nm)
N-Exo	153.7 ± 31.3	0.361	126.2
H-Exo	137.7 ± 25.0	0.501	141.7

21-5p in each sample was then analyzed. Relative quantification was obtained using the $2^{-\Delta\Delta Ct}$ method with hsa-miR-423-5p and hsa-miR-191-5p as endogenous controls, whose expression was known to be stable in hypoxia. As shown in Figure 6, the expression of hsa-miR-21-5p in H-Exo and N-Exo differed significantly, with a notable downregulation of hsa-miR-21-5p in H-Exo relative to its expression in N-Exo.

4. Discussion

This study highlights the utility of the ultrafiltration method for exosome enrichment and the impact of hypoxic conditioning on exosomal hsa-miR-21-5p expression. Confirmation of the presence of exosomes within samples obtained through ultrafiltration was conducted by testing the samples for exosome characteristics. In

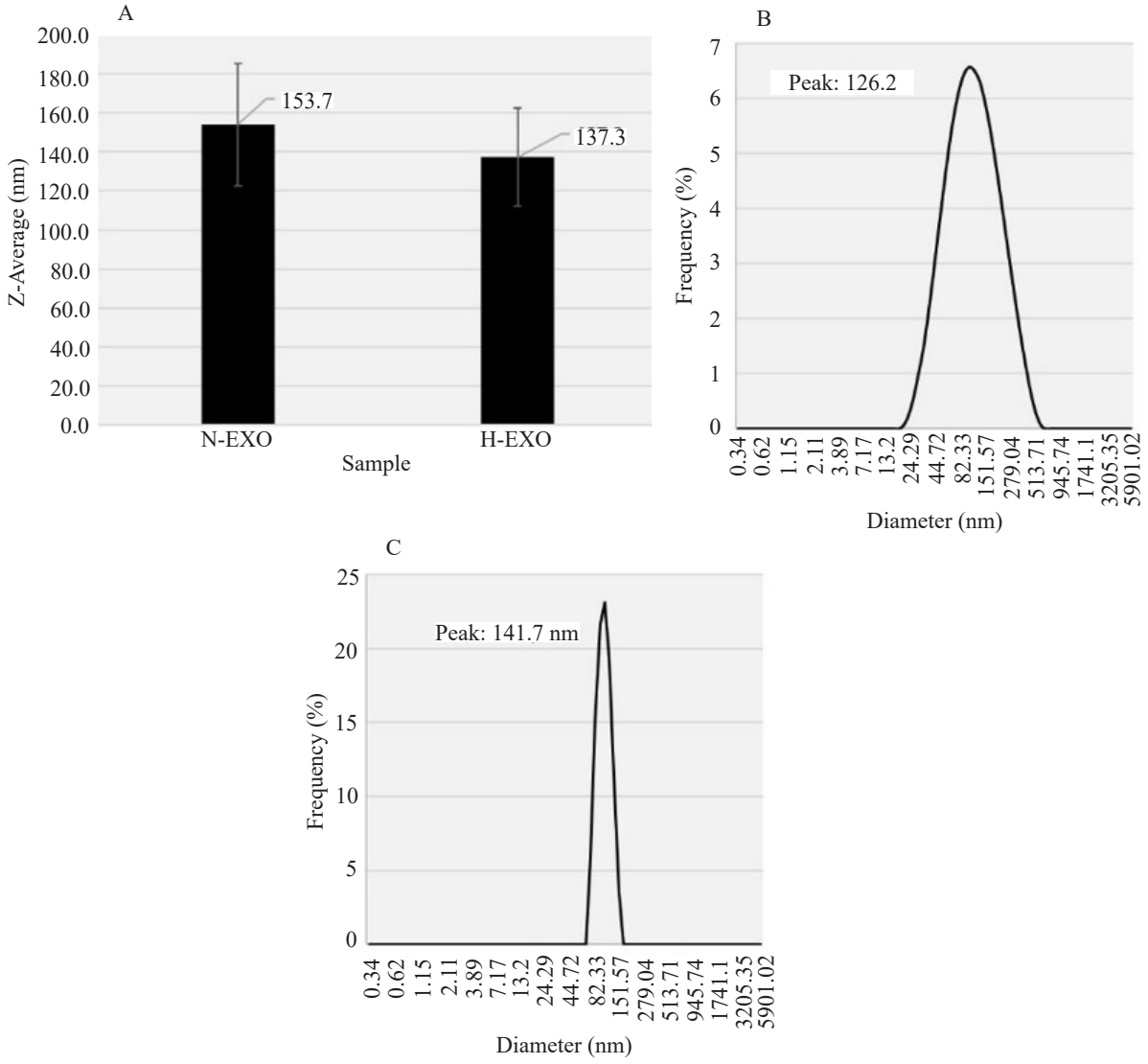

Figure 3. Z-average of N-Exo and H-Exo particles (A) as well as size distributions of particles in N-Exo (B) and H-Exo (C) based on Dynamic Light Scattering (DLS)

Table 2. Concentration of exosomes within samples based on Nanoparticle Tracking Analysis (NTA)

Samples	Concentration of particles within 30-150 nm (10^6 particles/ml)	Total particle concentration (10^6 particles/ml)
N-Exo	269	746
H-Exo	279	666

this study, exosome characterization was conducted in accordance with the recommendations from MISEV 2018 and involved testing for exosomal surface markers CD63 and CD81, morphological assessment using TEM imaging and DLS, as well as quantification using NTA. In addition, characterization was also supported by evaluation of internalization.

H-Exo and N-Exo samples were shown to contain exosomal surface markers CD63 and CD81. CD63 and CD81 are two tetraspanins often considered classic exosomal markers, with a two-decade history of use for exosome characterization (Mathieu *et al*. 2021). This is because these tetraspanins are known to be enriched in and are the most commonly identified proteins in exosomes. This is especially true for CD63, which has been consistently reported to be localized and found in abundance within the endosomal intracellular compartment (Andreu & Yáñez-Mó 2014). In the

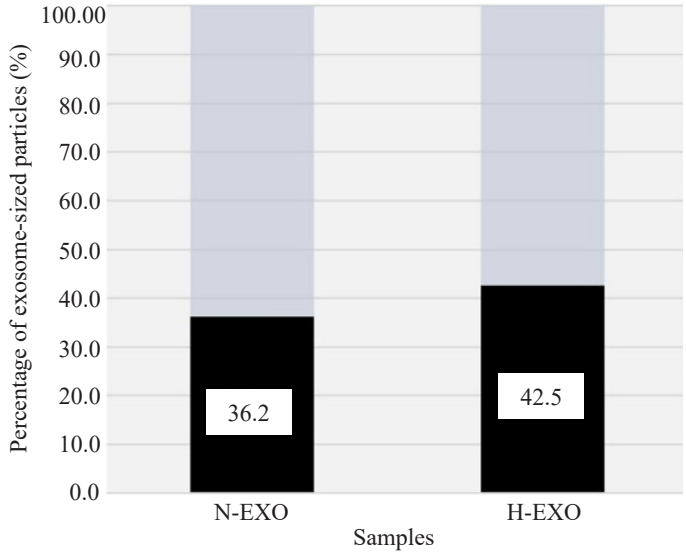

Figure 4. Percentage of particles 30-150 nm in size based on Nanoparticle Tracking Analysis (NTA)

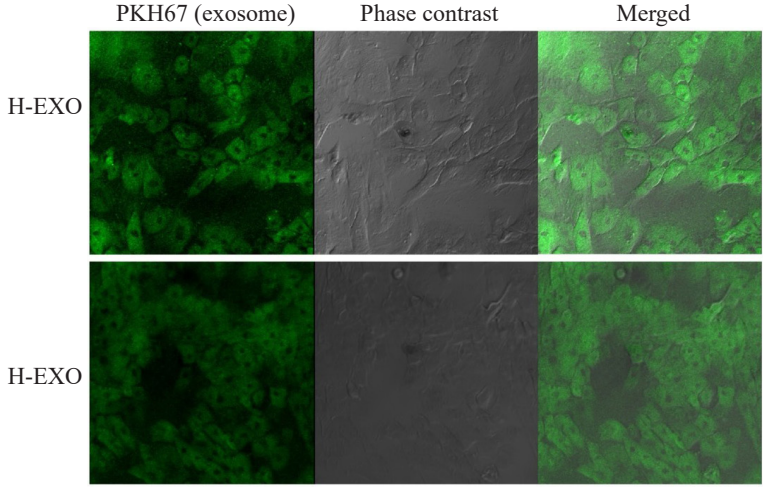

Figure 5. Confocal images depicting uptake of H-Exo and N-Exo in 20× Channels: PKH67, contrast phase, merged

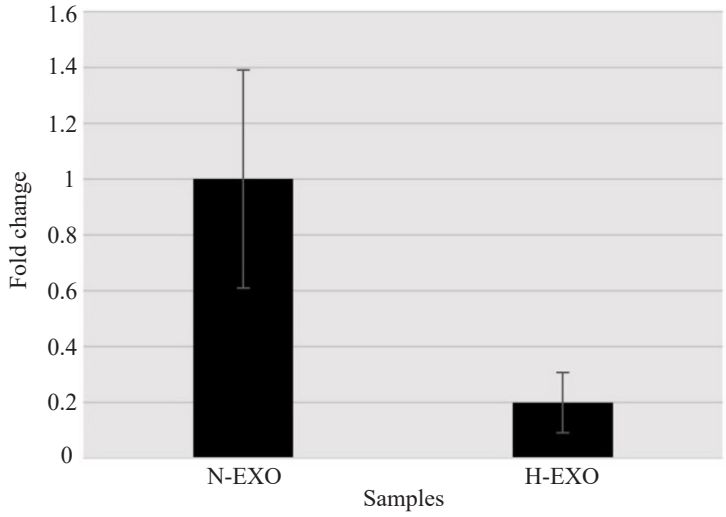

Figure 6. Relative expression of hsa-miR-21-5p with hsa-miR-191-5p and hsa-miR-423-5p as endogenous controls

majority of cells, CD63 can be found on lysosomes and multivesicular bodies (MVB), which, upon secretion by cells, release exosomes (Pols & Klumperman 2009). Therefore, the expression of tetraspannin CD63 and CD81 within all replicates of N-Exo and H-Exo indicates the prospective presence of exosomes within the respective samples.

The visualization results given in Figure 2 reveal the existence of morphologically circular and oval objects measuring 30-40 nm in each sample. The morphological description aligns with previous descriptions of exosomes (Colombo *et al*. 2014). The observed structures appear darker at the edges, indicating the accumulation of Uranyless dye on the background due to repulsion between the similarly negatively charged dye and phosphate groups of the phospholipid bilayer membrane in the exosome (Cao *et al*. 2011). This indicates the presence of particles with intact membranes (Shu *et al*. 2021), a key feature of exosomes that confirms the existence of particles morphologically consistent with the description of exosomes within the samples above.

As shown in Figure 3A, the Z-averages of N-Exo and H-Exo particles did not significantly differ. This finding aligns with other studies, in which MSCs cultured under hypoxic and normoxic conditions produced exosomes with similar size profiles (Liu *et al*. 2019; Yuan *et al*. 2021). To go into more detail, particles contained within representative samples of both N-Exo and H-Exo are polydisperse with PI>0.1 (Hughes *et al*. 2015) and range within 105.1-213.6 nm in size. Exosomes are a subpopulation of extracellular vesicles (EVs) with a size range of 30-150 nm, and a degree of heterogeneity is expected in samples (Colombo *et al*. 2014). The results obtained are also in line with other studies reporting polydisperse distributions with a polydispersity index (PI) of around 0.3. In addition, although the samples are polydisperse, the PI values are still within the optimal range for DLS readings (<0.7). However, DLS results do indicate the presence of particles outside the exosomal size range within samples, possibly due to the presence of larger EV subpopulations, such as microvesicles (MVs), or due to the formation of exosome aggregates. MV particles are known to have a certain degree of flexibility which allows them to pass through the 0.2 µm filters used in this study (Heinemann *et al*. 2014), and aggregates may form during dead-end filtration due to interaction of exosomes and other proteins in the sample with the membrane surface of filters (Sidhom *et al*. 2020). Exosomes may also aggregate when stored in physiological saline solutions (Bosch *et al*. 2016). However, particles with the highest frequencies in H-Exo and N-Exo are 141.7 nm and 126.2 nm in size, respectively, with average sizes of 153.7 ± 31.3 nm and 137.7 ± 25.0 nm. Thus, DLS readings of H-Exo and N-Exo indicate that a significant population of particles is within the exosomal size range.

The concentration of total particles, as well as the concentration of exosome-sized particles, determined through NTA, is quite low relative to the majority of studies involving exosome isolation. This may be due to the ultrafiltration method conducted in this study, which, while more practical and efficient to perform compared to the conventional ultracentrifugation method, has been reported to yield relatively lower amounts of exosome particles due to membrane blockage and the formation of aggregates (Alvarez *et al*. 2012; Yang *et al*. 2020). Although ultrafiltration may result in lower exosome yield, it has been shown to produce samples with a higher purity of exosomes (Konoshenko *et al*. 2018). This can also be observed in this study. Figure 4 shows that 36.2% and 42.6% of particles in the N-Exo and H-exo samples are exosomal in size, respectively (30-150 nm). On the one hand, this confirms the DLS readings, suggesting the presence of particles outside the exosomal size range, which has been discussed previously. On the other hand, this number is higher relative to exosome isolation by ultracentrifugation methods, which have been reported to generally yield samples with around 23% exosome-sized particles (Heinemann *et al*. 2014).

As additional characterization, the internalization of particles in representative samples of N-Exo and H-Exo was also assessed. Exosomes modulate physiological processes by transporting bioactive cargo and releasing it within target cells once they are internalized. As such, the capability of exosomes to be internalized is essential in the context of their use as therapeutic agents (Akers *et al*. 2013). Observation of both N-Exo and H-Exo samples using confocal microscopy, as shown in Figure 5, reveals the presence of PKH67 label exosomes within the cytosolic region of hWJ-MSC cells. Although some signals were detected within the extracellular region, within one hour, exosome particles have begun to internalize into hWJ-MSC cells. Exosomes are known to be internalized through a variety of routes, including fusion with the plasma membrane, clathrin-dependent endocytosis pathways, as well as clathrin-independent pathways such as macropinocytosis and lipid raft-mediated endocytosis (Dominkuš *et al*. 2018). Various studies have also previously reported the uptake of MSC-derived exosomes by various cells ranging from

somatic cells such as fibroblasts (Bakhtyar *et al*. 2018), endothelial cells (Gong *et al*. 2017) and cardiomycocytes (Liang *et al*. 2021), to cancer cell lines (Karaoz *et al*. 2019).

Thus, samples containing particles with characteristics that match the description of exosomes have been successfully obtained through ultrafiltration. Representative samples of both H-Exo and N-Exo were found to contain particles expressing CD81 and CD63 exosomal markers, which possess morphologies and size ranges of exosomes classically described in literature. Particles within both samples were also shown to be capable of internalization by hWJ-MSC cells.

The expression of hsa-miR-21-5p in H-Exo and N-Exo differed, with H-Exo exhibiting considerable downregulation compared to N-Exo. This suggests that hypoxic conditioning on hUC-MSCs led to a decrease in hsa-miR-21-5p expression contained within MSC-derived exosomes. miRNA expression levels in exosomes are known to correlate with their expression within source cells. The reduction in exosomal hsa-miR-21-5p might be due to a decrease in hsa-miR-21-5p expression in cells. It was previously reported that hypoxia may have varying effects on hsa-miR-21-5p expression. Prolonged hypoxic treatment (> 60 minutes) on cardiomycocytes was reported to suppress hsa-miR-21-5p expression, however a relatively short period of hypoxia (15 minutes) increased its expression (Sayed *et al*. 2010). Expression of hsa-miR-21-5p under hypoxic conditions is regulated through a mechanism that is HIF-independent, namely through the action of protein kinase B (AKT). Prolonged hypoxia may induce the dephosphorylation and deactivation of AKT. However, this deactivation depends on the presence of phosphatase and tensin homolog deleted on chromosome 10 (PTEN). It is rarely observed in specific cells that are deficient in PTEN, such as cancer cell lines SW480 and MCF-7. In these cells, exposure to hypoxia of over 48 hours did not decrease hsa-miR-21-5p expression (Dong *et al*. 2019). Therefore, the impact of hypoxic conditioning on the expression of hsa-miR-21-5p is affected by several factors, such as the length of exposure and the source cells involved, and thus further research is needed to determine whether this model applies to the hUC-MSC cells, such as the ones used in this study.

The study of hsa-miR-21-5p expression under hypoxic conditions is generally centered around exosomes from cancerous cell lines, where hypoxic conditioning tends to cause upregulation of hsa-miR-21-5p. Studies regarding the expression of hsa-miR-21-5p have not been conducted very much. However, Zhang *et al*. (2021) have reported hsa-miR-21-5p as one of the miRNAs whose expression was upregulated in hypoxic MSC exosomes. However, there were also studies that did not report an increase in hsa-miR-21-5p in hypoxic MSC-derived exosomes. The difference in results obtained through this study compared to those conducted by Zhang *et al*. (2021) may be due to variations in the hypoxic conditioning methods used. In this study, expansion and culture of hUC-MSC cells from the working cell bank to the 5th passage were carried out under hypoxic conditions (5% O_2).

Meanwhile, the referenced study incubated cells in hypoxic conditions for 3-6 hours (1% O_2). As mentioned previously, duration of exposure plays a role in determining the effect of hypoxia on hsa-miR-21-5p expression. The difference in oxygen saturation may also play a role, as the 5% O_2 levels were to mimic MSC niches in vivo, and 1% O_2 levels were to simulate the stressful conditions of a skin injury. The media composition used for MSC culture by Zhang *et al*. (2021) is also slightly different from that used in this study. Zhang *et al*. (2021) cultured their cells in DMEM, while this study utilized MEM-α. The various compositions of the two culture media might create a slightly different microenvironment, which plays a role in determining the function and fate of MSCs (Haque *et al*. 2013). Additionally, other factors, such as cell passage number, may also influence the results. Zhang *et al*. (2021) did not disclose the cell passage number for the MSCs used in their study; however, the passage number may affect a cell line's characteristics over time, including alterations to its response to stimuli and protein expression. It was also reported that MSCs from different passages may have varying cytokine secretion capacities (Carmona-Luque *et al*. 2024), which may consequently affect their immunomodulatory properties.

Overall, this study found that H-Exo and N-Exo contained particles that matched the size, morphology, and surface protein expression of exosomes. Samples also contained particles that were rapidly taken up by cells. The yield of exosomes in this study was low, but it had a higher percentage of exosomes compared to conventional ultracentrifugation methods. Hypoxic conditioning of hUC-MSCs did not affect the size profile or morphology of exosomes, but resulted in downregulation of exosomal hsa-miR-21-5p expression. Considering that hsa-miR-21-5p is one of the cargoes which mediates exosome immunomodulatory activity, the results of this study can be used as a consideration in determining the appropriate cellular conditioning for future production of exosomes as a therapeutic agent.

However, it is also worth noting that this study has its own limitations. This study was intended as an initial examination of the potential of hypoxic conditioning to increase the anti-inflammatory activity of hUC-MSC-derived exosomes; therefore, certain procedures were conducted only to the extent necessary to provide preliminary information. In this study, the anti-inflammatory potential of N-Exo and H-Exo were solely assessed through expression level of hsa-miR-21-5p. Although sufficient to provide initial evidence of the effect of hypoxic conditioning on exosomal hUC-MSC, a more exhaustive evaluation comprising other components of the exosomal cargo would be beneficial to confirm the decrease in anti-inflammatory activity observed from the hypoxic conditioning conducted in this study. Furthermore, this study has also yet to investigate the effects of longer durations of hypoxic conditioning. With the knowledge that the duration of hypoxic conditions might play a significant role in affecting exosomal MSC, future research can be conducted to compare several different durations of hypoxic conditioning. As therapeutic applications require the therapeutic agent to be reliably produced at a large scale, it will be of considerable interest to investigate and compare the yields of different exosome isolation/enrichment methods, particularly since exosome yield can be considered relatively low using the ultrafiltration method conducted in this study. The characterizations undertaken in this study would also benefit from the added robustness of additional testing for other surface markers such as TSG101 and ALIX.

Acknowledgements

This research was supported by the Stem Cell and Cancer Institute and Institut Teknologi Bandung (Riset ITB-Unggulan no.148/IT1.1307.1/TA.00/2021), as well as by PT Wadya Prima Mulia and Evident Scientific Singapore PTE. LTD., with confocal imaging being performed at Scientific Imaging Center ITB using the FV1200. We would also like to thank Safira Meidina Nursatya and Andika Ardiyansyah for preparing and proofreading the article.

References

Akers, J.C., Gonda, D., Kim, R., Carter, B.S., Chen, C.C., 2013. Biogenesis of extracellular vesicles (EV): exosomes, microvesicles, retrovirus-like vesicles, and apoptotic bodies. *Journal of Neuro-Oncology*. 113, 1-11. https://doi.org/10.1007/s11060-013-1084-8

Alvarez, M.L., Khosroheidari, M., Kanchi Ravi, R., DiStefano, J.K., 2012. Comparison of protein, microRNA, and mRNA yields using different methods of urinary exosome isolation for the discovery of kidney disease biomarkers. *Kidney International*. 82, 1024-1032. https://doi.org/10.1038/ki.2012.256

Andreu, Z., Yáñez-Mó, M., 2014. Tetraspanins in extracellular vesicle formation and function. *Frontiers in Immunology*. 5. https://doi.org/10.3389/fimmu.2014.00442

Bai, L., Lennon, D.P., Caplan, A.I., DeChant, A., Hecker, J., Kranso, J., Zaremba, A. and Miller, R.H., 2012. Hepatocyte growth factor mediates mesenchymal stem cell–induced recovery in multiple sclerosis models. *Nature Neuroscience*. 15, 862-870. doi:https://doi.org/10.1038/nn.3109.

Bakhtyar, N., Jeschke, M.G., Herer, E., Sheikholeslam, M., Amini-Nik, S., 2018. Exosomes from acellular Wharton's jelly of the human umbilical cord promotes skin wound healing. *Stem Cell Research & Therapy*. 9. https://doi.org/10.1186/s13287-018-0921-2

Bosch, S., de Beaurepaire, L., Allard, M., Mosser, M., Heichette, C., Chrétien, D., Jegou, D., Bach, J.M., 2016. Trehalose prevents aggregation of exosomes and cryodamage. *Scientific Reports*. 6. https://doi.org/10.1038/srep36162

Cao, B., Xu, H., Mao, C., 2011. Transmission electron microscopy as a tool to image bioinorganic nanohybrids: The case of phage-gold nanocomposites. *Microscopy Research and Technique*. 74, 627-635. https://doi.org/10.1002/jemt.21030

Carmona-Luque, M.d., Ballesteros-Ribelles, A., Millán-López, A., Blanco, A., Nogueras, S., Herrera, C., 2024. The Effect of cell culture passage on the efficacy of mesenchymal stromal cells as a cell therapy treatment. *Journal of Clinical Medicine*. 13, 2480-2480. doi:https://doi.org/10.3390/jcm13092480.

Cha, J.M., Shin, E.K., Sung, J.H., Moon, G.J., Kim, E.H., Cho, Y.H., Park, H.D., Bae, H., Kim, J., Bang, O.Y., 2018. Efficient scalable production of therapeutic microvesicles derived from human mesenchymal stem cells. *Scientific Reports*. 8. https://doi.org/10.1038/s41598-018-19211-6

Colombo, M., Raposo, G., Théry, C., 2014. Biogenesis, secretion, and intercellular interactions of exosomes and other extracellular vesicles. *Annual Review of Cell and Developmental Biology*. 30, 255-289. https://doi.org/10.1146/annurev-cellbio-101512-122326

Dominkuš, P.P., Stenovec, M., Sitar, S., Lasič, E., Zorec, R., Plemenitaš, A., Žagar, E., Kreft, M., Lenassi, M., 2018. PKH26 labeling of extracellular vesicles: Characterization and cellular internalization of contaminating PKH26 nanoparticles. *Biochimica et Biophysica Acta (BBA)-Biomembranes*. 1860, 1350-1361. https://doi.org/10.1016/j.bbamem.2018.03.013

Dong, C., Liu, X., Wang, H., Li, J., Dai, L., Li, J., Xu, Z., 2019. Hypoxic non-small-cell lung cancer cell-derived exosomal miR-21 promotes resistance of normoxic cell to cisplatin. *OncoTargets and Therapy*. 12, 1947-1956. https://doi.org/10.2147/ott.s186922

Giovannelli, L., Bari, E., Jommi, C., Tartara, F., Armocida, D., Garbossa, D., Cofano, F., Torre, M.L., Segale, L., 2023. Mesenchymal stem cell secretome and extracellular vesicles for neurodegenerative diseases: Risk-benefit profile and next steps for the market access. *Bioactive Materials*. 29, 16-35. doi:https://doi.org/10.1016/j.bioactmat.2023.06.013.

Gong, M., Yu, B., Wang, J., Wang, Y., Liu, M., Paul, C., Millard, R. W., Xiao, D.-S., Ashraf, M., Xu, M., 2017. Mesenchymal stem cells release exosomes that transfer miRNAs to endothelial cells and promote angiogenesis. *Oncotarget*. 8, 45200-45212. https://doi.org/10.18632/oncotarget.16778

Haque, N., Rahman, M.T., Abu Kasim, N.H., Alabsi, A.M., 2013. Hypoxic Culture Conditions as a Solution for Mesenchymal Stem Cell Based Regenerative Therapy. *The Scientific World Journal*. 2013. doi:https://doi.org/10.1155/2013/632972.

Harrell, C.R., Jovicic, N., Djonov, V., Arsenijevic, N., Volarevic, V., 2019. Mesenchymal stem cell-derived exosomes and other extracellular vesicles as new remedies in the therapy of inflammatory diseases. *Cells*. 8, 1605. https://doi.org/10.3390/cells8121605

Heinemann, M.L., Ilmer, M., Silva, L.P., Hawke, D.H., Recio, A., Vorontsova, M.A., Alt, E., Vykoukal, J., 2014. Benchtop isolation and characterization of functional exosomes by sequential filtration. *Journal of Chromatography A*, 1371, 125-135. https://doi.org/10.1016/j.chroma.2014.10.026

Hou, Y., Li, J., Guan, S., Witte, F., 2021. The therapeutic potential of MSC-EVs as a bioactive material for wound healing. *Engineered Regeneration*, 2, 182-194. https://doi.org/10.1016/j.engreg.2021.11.003

Hughes, J. M., Budd, P. M., Grieve, A., Dutta, P., Tiede, K., Lewis, J., 2015. Highly monodisperse, lanthanide-containing polystyrene nanoparticles as potential standard reference materials for environmental "nano" fate analysis. *Journal of Applied Polymer Science*. 132, 1-9. https://doi.org/10.1002/app.42061

Ji, J., Sundquist, J., Sundquist, K., 2016. Gender-specific incidence of autoimmune diseases from national registers. *Journal of Autoimmunity*. 69, 102-106. https://doi.org/10.1016/j.jaut.2016.03.003

Karaoz, E., Sun, E., Demir, C.S., 2019. Mesenchymal stem cell-derived exosomes do not promote the proliferation of cancer cells *in vitro*. *International Journal of Physiology, Pathophysiology and Pharmacology*. 11, 177-189.

Konoshenko, M.Yu., Lekchnov, E.A., Vlassov, A.v, Laktionov, P.P., 2018. Isolation of extracellular vesicles: general methodologies and latest trends. *BioMed Research International*. 2018, 1-27. https://doi.org/10.1155/2018/8545347

Liang, C., Liu, Y., Xu, H., Huang, J., Shen, Y., Chen, F., Luo, M., 2021. Exosomes of human umbilical cord MSCs protect against hypoxia/reoxygenation-induced pyroptosis of cardiomyocytes via the miRNA-100-5p/FOXO3/NLRP3 pathway. *Frontiers in Bioengineering and Biotechnology*. 8. https://doi.org/10.3389/fbioe.2020.615850

Liu, H., Sun, X., Gong, X., Wang, G., 2019. Human umbilical cord mesenchymal stem cells derived exosomes exert antiapoptosis effect via activating PI3K/Akt/mTOR pathway on H9C2 cells. *Journal of Cellular Biochemistry*. https://doi.org/10.1002/jcb.28705

Mathieu, M., Névo, N., Jouve, M., Valenzuela, J.I., Maurin, M., Verweij, F.J., Palmulli, R., Lankar, D., Dingli, F., Loew, D., Rubinstein, E., Boncompain, G., Perez, F., Théry, C., 2021. Specificities of exosome versus small ectosome secretion revealed by live intracellular tracking of CD63 and CD9. *Nature Communications*. 12. https://doi.org/10.1038/s41467-021-24384-2

McCaughan, G., 2004. Molecular approaches to the side effects of immunosuppressive drugs. *Transplantation*. 78, 1114-1115. https://doi.org/10.1097/01.tp.0000137263.30162.6b

Nowak-Stępniowska, A., Osuchowska, P.N., Fiedorowicz, H., Trafny, E.A., 2022. Insight in hypoxia-mimetic agents as potential tools for mesenchymal stem cell priming in regenerative medicine. *Stem Cells International*. 2022, 1-24. https://doi.org/10.1155/2022/8775591

Pols, M.S., Klumperman, J., 2009. Trafficking and function of the tetraspanin CD63. *Experimental Cell Research*. 315, 1584-1592. https://doi.org/10.1016/j.yexcr.2008.09.020

Regmi, S., Pathak, S., Kim, J.O., Yong, C.S., Jeong, J.H., 2019. Mesenchymal stem cell therapy for the treatment of inflammatory diseases: Challenges, opportunities, and future perspectives. *European Journal of Cell Biology*. 98, 151041. https://doi.org/10.1016/j.ejcb.2019.04.002

Sayed, D., He, M., Hong, C., Gao, S., Rane, S., Yang, Z., Abdellatif, M., 2010. MicroRNA-21 is a downstream effector of AKT that mediates its antiapoptotic effects via suppression of fas ligand. *Journal of Biological Chemistry*. 285, 20281-20290. https://doi.org/10.1074/jbc.m110.109207

Sheedy, F.J., 2015. Turning 21: Induction of miR-21 as a key switch in the inflammatory response. *Frontiers in Immunology*. 6. https://doi.org/10.3389/fimmu.2015.00019

Shu, S.la., Allen, C.L., Benjamin-Davalos, S., Koroleva, M., MacFarland, D., Minderman, H., Ernstoff, M.S., 2021. A rapid exosome isolation using ultrafiltration and size exclusion chromatography (REIUS) method for exosome isolation from melanoma cell lines. *Methods in Molecular Biology*. 2265, 289-304. https://doi.org/10.1007/978-1-0716-1205-7_22

Sidhom, K., Obi, P.O., Saleem, A., 2020. A review of exosomal isolation methods: Is size exclusion chromatography the best option? *International Journal of Molecular Sciences*. 21, 6466. https://doi.org/10.3390/ijms21186466

Soler-Botija, C., Monguió-Tortajada, M., Munizaga-Larroudé, M., Gálvez-Montón, C., Bayes-Genis, A., Roura, S., 2022. Mechanisms governing the therapeutic effect of mesenchymal stromal cell-derived extracellular vesicles: A scoping review of preclinical evidence. *Biomedicine & Pharmacotherapy*. 147, 112683. https://doi.org/10.1016/j.biopha.2022.112683

Song, N., Zhang, T., Xu, X., Lu, Z., Yu, X., Fang, Y., Hu, J., Jia, P., Teng, J., Ding, X., 2018. miR-21 protects against ischemia/reperfusion-induced acute kidney injury by preventing epithelial cell apoptosis and inhibiting dendritic cell maturation. *Frontiers in Physiology*. 9. https://doi.org/10.3389/fphys.2018.00790

Tabas, I., Glass, C.K., 2013. Anti-inflammatory therapy in chronic disease: challenges and opportunities. *Science*. 339, 166-172. https://doi.org/10.1126/science.1230720

Théry, C., Witwer, K.W., Aikawa, E., Alcaraz, M.J., Anderson, J. D., Andriantsitohaina, R., Antoniou, A., Arab, T., Archer, F., Atkin-Smith, G.K., Ayre, D.C., Bach, J.M., Bachurski, D., Baharvand, H., Balaj, L., Baldacchino, S., Bauer, N. N., Baxter, A.A., Bebawy, M., … Zuba-Surma, E.K., 2018. Minimal information for studies of extracellular vesicles 2018 (MISEV2018): a position statement of the International Society for Extracellular Vesicles and update of the MISEV2014 guidelines. *Journal of Extracellular Vesicles*. 7, 1535750. https://doi.org/10.1080/20013078.2018.1535750

Wang, Y., Chen, X., Cao, W., Shi, Y., 2014. Plasticity of mesenchymal stem cells in immunomodulation: pathological and therapeutic implications. *Nature Immunology*. 15, 1009-1016. https://doi.org/10.1038/ni.3002

Yang, L., Wang, B., Zhou, Q., Wang, Y., Liu, X., Liu, Z., & Zhan, Z., 2018. MicroRNA-21 prevents excessive inflammation and cardiac dysfunction after myocardial infarction through targeting KBTBD7. *Cell Death & Disease*. 9. https://doi.org/10.1038/s41419-018-0805-5

Yang, D., Zhang, W., Zhang, H., Zhang, F., Chen, L., Ma, L., Larcher, L. M., Chen, S., Liu, N., Zhao, Q., Tran, P. H. L., Chen, C., Veedu, R. N., Wang, T., 2020. Progress, opportunity, and perspective on exosome isolation - efforts for efficient exosome-based theranostics. *Theranostics*. 10, 3684-3707. https://doi.org/10.7150/thno.41580

Yuan, N., Ge, Z., Ji, W., Li, J., 2021. Exosomes secreted from hypoxia-preconditioned mesenchymal stem cells prevent steroid-induced osteonecrosis of the femoral head by promoting angiogenesis in rats. *BioMed Research International*. 2021, 1-13. https://doi.org/10.1155/2021/6655225

Zhang, X.-F., Wang, T., Wang, Z.-X., Huang, K.-P., Zhang, Y.-W., Wang, G.-L., Zhang, H.-J., Chen, Z.-H., Wang, C.-Y., Zhang, J.-X., Wang, H., 2021. Hypoxic ucMSC-secreted exosomal miR-125b promotes endothelial cell survival and migration during wound healing by targeting TP53INP1. *Molecular Therapy - Nucleic Acids*. 26, 347-359. https://doi.org/10.1016/j.omtn.2021.07.014

Zhou, W., Su, L., Duan, X., Chen, X., Hays, A., Upadhyayula, S., Shivde, J., Wang, H., Li, Y., Huang, D., Liang, S., 2018. MicroRNA-21 down-regulates inflammation and inhibits periodontitis. *Molecular Immunology*, 101, 608-614. https://doi.org/10.1016/j.molimm.2018.05.008